RESEARCH ARTICLE

Theoretical Investigation on the Copper-Catalyzed *anti*-Selective 1,2-Silylboration of Internal Alkynes

Hirokazu Moniwa,[a] Masahiro Yamanaka,*[b] and Ryo Shintani,*[a,c]

[a] H. Moniwa, Prof. Dr. R. Shintani
Division of Chemistry, Department of Materials Engineering Science, Graduate School of Engineering Science, Osaka University
Toyonaka, Osaka 560-8531 (Japan)
E-mail: shintani.ryo.es@osaka-u.ac.jp

[b] Prof. Dr. M. Yamanaka
Department of Chemistry and Research Center for Smart Molecules, Faculty of Science, Rikkyo University
Toshima-ku, Tokyo 171-8501 (Japan)
E-mail: myamanak@rikkyo.ac.jp

[c] Prof. Dr. R. Shintani
Innovative Catalysis Science Division, Institute for Open and Transdisciplinary Research Initiatives (ICS-OTRI), Osaka University
Suita, Osaka 565-0871 (Japan)

Supporting information for this article is given via a link at the end of the document.

Abstract: The mechanism of a copper-catalyzed regio- and *anti*-selective 1,2-silylboration of internal alkynes was theoretically studied to understand the reaction pathway and the origin of selectivity. The proposed overall reaction pathway involves the *syn*-to-*anti* isomerization via an anionic allenic transition state stabilized by the conjugation with the benzene ring. The *anti*-selectivity is determined at the borylation step and controlled by the steric effect of the silyl group introduced on the alkyne carbon. The computational results obtained in this study are highly informative for the development of new catalytic transformations involving *syn*/*anti*-isomerization processes.

Introduction

1,2-Addition reactions to a carbon–carbon triple bond of alkynes are efficient and straightforward ways to synthesize substituted alkenes. In these reactions, both regioselectivity and stereoselectivity are important factors to determine the structure of resulting alkene products. In particular, *syn*-selective reactions typically take place for both hydrofunctionalization[1] and difunctionalization[2] under transition-metal catalysis, but *anti*-selective reactions can be realized by using π-acidic metal catalysts,[2d,f,3] involvement of radical intermediates,[2b,d,3c] or going through *syn*-to-*anti* isomerization of the initially formed *syn*-alkenylmetal intermediates.[2a,b,d,e]

In the *anti*-selective reactions via *syn*-to-*anti* isomerization, the detailed mechanism and its driving force are of high interest to understand the origin of selectivity and thereby to develop new and useful synthetic transformations. In this regard, some representative mechanisms have been described in the pioneering work on the rhodium-[4] or iridium-catalyzed[5] *anti*-selective hydrosilylation of terminal alkynes (Scheme 1). For example, Ojima and coworkers proposed the isomerization of a *syn*-silylalkenylrhodium intermediate to its *anti*-form through a zwitterionic rhodium carbene species, and the preferential formation of the *anti*-hydrosilylation product was explained by

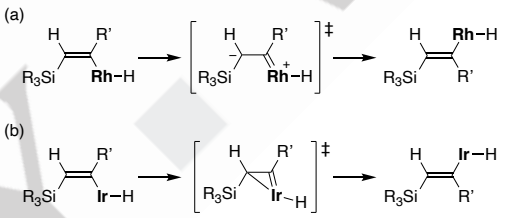

Scheme 1. Proposed reaction pathways for *syn*-to-*anti* isomerization in the (a) rhodium- and (b) iridium-catalyzed hydrosilylation of terminal alkynes.

avoidance of unfavorable steric repulsion between the silyl group and the rhodium moiety.[4b] On the other hand, Tanke and Crabtree proposed the isomerization of *syn*-silylalkenyliridium intermediate via an η^2-vinyliridium (iridacyclopropene) to give *anti*-hydrosilylation products.[5a]

More recently, with the aid of advancement of computational chemistry, detailed mechanisms of *syn*-to-*anti* isomerization of alkenylmetal species have been described using DFT calculations in the context of various transition-metal-catalyzed *anti*-selective addition reactions of alkynes, including the catalyst systems based on nickel,[6] palladium,[7] rhodium,[8] iridium,[9] and ruthenium.[10] In most of these cases, involvement of η^2-vinylmetal (metalacyclopropene) species was suggested as the plausible transition state for the *syn*-to-*anti* isomerization. On the other hand, although multiple examples are known for the copper-catalyzed *anti*-addition to alkynes[11] and some of them proposed the involvement of *syn*-to-*anti* isomerization,[11c,i] no detailed mechanistic investigations on *syn*-to-*anti* isomerization of alkenylcopper intermediates have been reported to date as far as we are aware.

In this context, we previously developed a copper-catalyzed regio- and *anti*-selective 1,2-silylboration of internal alkyl(aryl)acetylenes to give silicon- and boron-containing tetrasubstituted alkenes presumably via *syn*-to-*anti* isomerization of the initially formed *syn*-silylalkenylcopper intermediate.[12,13] To understand the details of this process, herein we conducted DFT calculations and found that the regioselectivity is determined by

both electronic and steric effects at the alkyne insertion step, that the *syn*-to-*anti* isomerization takes place reversibly via an anionic allenic transition state stabilized by the conjugation with the benzene ring, and that the *anti*-selectivity is determined by the steric effect at the borylation step.

Computational Details

All calculations were performed with the Gaussian 16 package.[14] Geometries were fully optimized and the energies were estimated by the DFT-B3LYP functional[15] using LANL2DZ for Cu, 6-31G(d) for C, H, B, O, Na atoms, and 6-31+G(d) for Si atom, including the solvation effect with the SCRF-SMD model using THF solvent.[16] Frequency analyses were carried out to confirm that each structure was a local minimum (no imaginary frequency) or a transition state (only one imaginary frequency).

Results and Discussion

In our previous study on the development of a copper-catalyzed silylboration of internal alkynes [Eq. (1)],[12a] the following results were obtained. (1) For the reaction of alkyl(aryl)acetylenes, high regioselectivity was achieved to give (1-boryl-2-silyl-1-alkenyl)arenes, and (2) high stereoselectivity was achieved to give *anti*-silylboration products. Both (1) and (2) were realized regardless of the size of alkyl groups and representative results are shown in Eq. (1). In our related study,[17] it was also suggested that (3) a disilylcuprate, not a neutral silylcopper(I), is the catalytically active species, and (4) the reaction proceeds through *syn*-insertion of an alkyne to the silicon–copper bond. (3) was further confirmed by a series of stoichiometric reactions using 1-phenyl-1-propyne (methyl(phenyl)acetylene; **1a**) with (dimethylphenylsilyl)boronate **2** as summarized in Figure S1 in the Supporting Information. Based on these data, a proposed catalytic cycle for the reaction of **1a** with **2** is shown in Scheme 2. Thus, disilylcuprate **A** undergoes regioselective *syn*-insertion of alkyne **1a** to give *syn*-alkenyl(silyl)cuprate **B**. Instead of direct borylation of **B** giving *syn*-**3a**, *syn*-to-*anti* isomerization of **B** takes place to give *anti*-alkenyl(silyl)cuprate **C**, which then reacts with silylboronate **2** to give silylboration product *anti*-**3a** along with regeneration of disilylcuprate **A**.

In contrast, our further investigation newly revealed that the use of dialkylacetylenes such as 3-hexyne (**1d**) and 5-decyne (**1e**) led to the formation of *syn*-addition products such as *syn*-**3d** and *syn*-**3e** with no formation of the corresponding *anti*-adducts [Eq. (2)]. These results suggest that the *syn*-to-*anti* isomerization (**B** → **C** in Scheme 2) may require an aryl substituent on the alkyne substrate. To understand the origin of this substituent effect on stereoselectivity of silylboration as well as the overall reaction pathway highlighting the *syn*-to-*anti* isomerization process, we conducted DFT calculations.

Based on the proposed catalytic cycle, the energy profile of the overall reaction pathway of the regio- and *anti*-selective 1,2-silylboration of alkyne **1a** with **2** was obtained (Scheme 3). The first step in Scheme 2, the insertion of alkyne **1a** to disilylcuprate

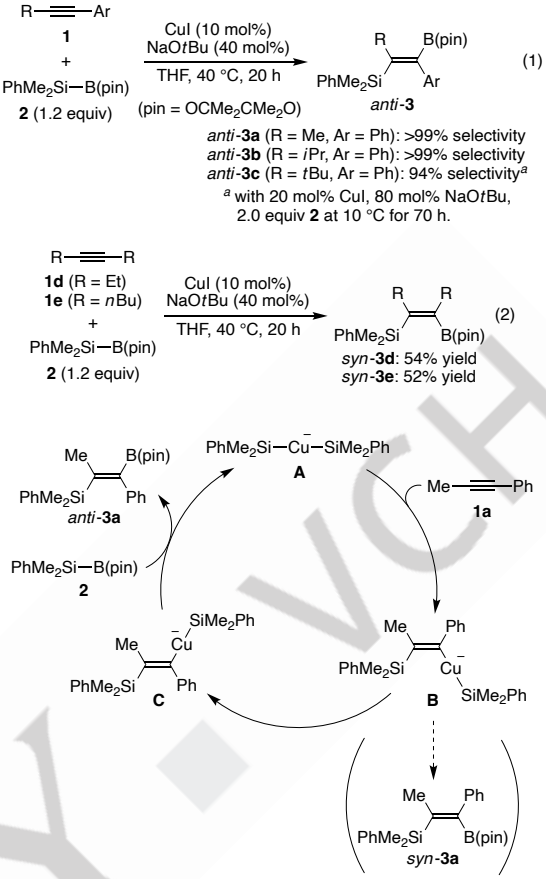

Scheme 2. Proposed catalytic cycle for the copper-catalyzed reaction of alkyne **1a** with silylboronate **2** to give *anti*-**3a**.

A, was initially investigated with a focus on the regioselectivity. The reaction of **1a** with **A** toward *syn*-alkenyl(silyl)cuprate **B** is exergonic by 24.9 kcal mol^{-1} via **TS A–B** ($\Delta G^{\ddagger}$ = 15.5 kcal mol^{-1}). The reaction with the opposite regioselectivity needs to go through energetically higher **TS A–B'** ($\Delta G^{\ddagger}$ = 21.1 kcal mol^{-1}) to give its regioisomer **B'** (–22.1 kcal mol^{-1}). This indicates that the formation of **B** is energetically more favorable than **B'**, which is in good agreement with the experimentally observed regioselectivity. Comparison of the transition-state structures between **TS A–B** and **TS A–B'** showed that **TS A–B** retains a stronger conjugate nature of the alkyne with the phenyl group in **1a** than **TS A–B'** (C1–C3 = 1.45 Å for **TS A–B** vs. C1–C3 = 1.47 Å for **TS A–B'**; Figure 1). In addition, **TS A–B** is sterically more favorable than **TS A–B'** due to the smaller steric repulsion with the incoming dimethylphenylsilyl group (∠C2–C1–Cu–Si = 23.9° for **TS A–B** vs. ∠C1–C2–Cu–Si = 28.3° for **TS A–B'**). Thus, the energy difference between **TS A–B** and **TS A–B'** is caused by both electronic and steric effects, leading to the preferential attack of a silicon nucleophile at the β-position to the phenyl group.

We then explored the key *syn*-to-*anti* isomerization step from **B** to **C**. Unlike the previously reported processes with other transition metals, we could not identify the transition states with zwitterionic metal carbene or η^2-vinylmetal structures (path 1 in Scheme 4). Instead, an anionic allenic structure stabilized by the benzene ring was found as a possible transition state (path 2 in Scheme 4). However, the energy barrier from **B** to **C** through this

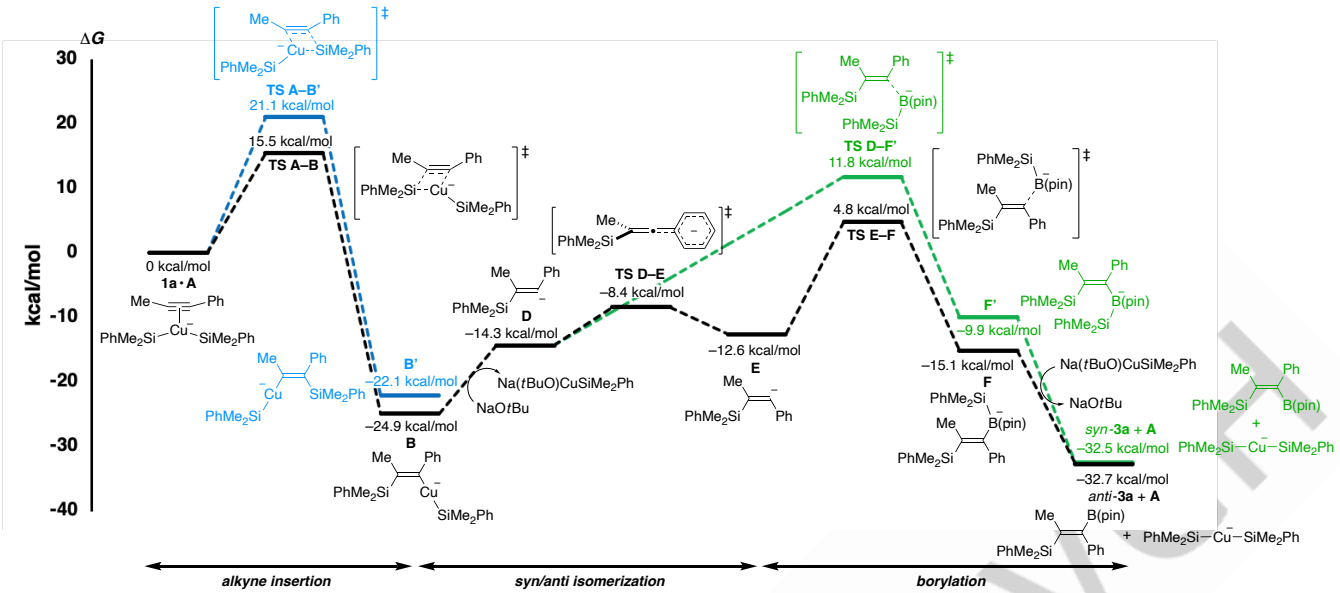

Scheme 3. Calculated reaction pathways for the reaction of **1a** with **2**.

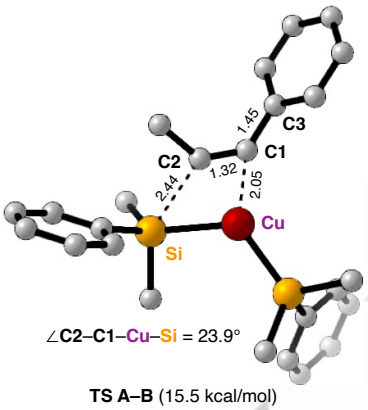

TS A–B (15.5 kcal/mol)

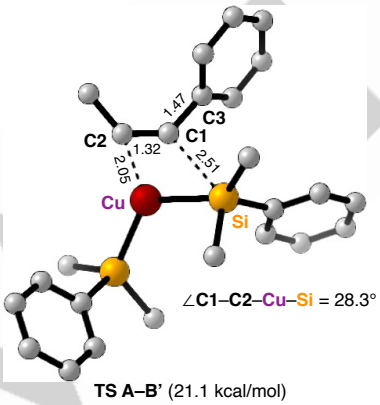

TS A–B' (21.1 kcal/mol)

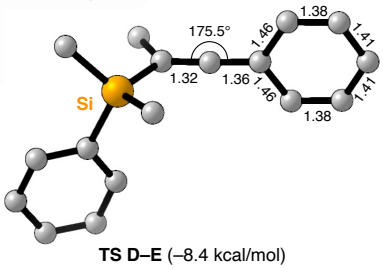

TS D–E (–8.4 kcal/mol)

Figure 1. Structures of **TS A–B**, **TS A–B'**, and **TS D–E**. Bond lengths are in Å.

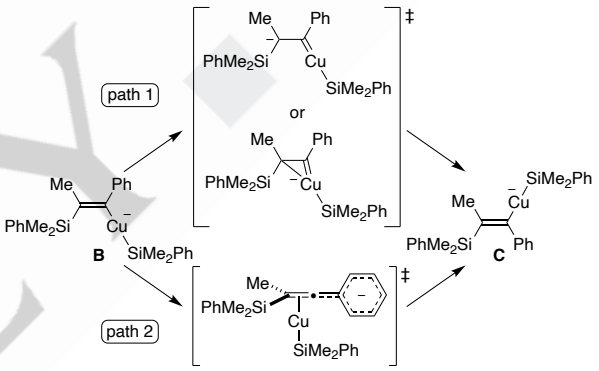

Scheme 4. Possible reaction pathways from **B** to **C**.

pathway was somewhat high ($\Delta G^{\ddagger}$ = 27.4 kcal mol^{-1}), and the subsequent borylation of **C** required even higher $\Delta G^{\ddagger}$ of 38.2 kcal mol^{-1}, although it is lower by 7.2 kcal mol^{-1} than the barrier for direct borylation of **B** to give *syn*-**3a** (Scheme S1 in the Supporting Information).

This promising but not exactly convincing isomerization pathway prompted us to further exploration of more plausible scenarios. As a result, it was found that dissociation of the silylalkenyl moiety from (dimethylphenylsilyl)copper gives more configurationally labile anionic species **D** (–14.3 kcal mol^{-1}; Scheme 3). This then undergoes isomerization to **E** (–12.6 kcal mol^{-1}) with a much lower barrier of $\Delta G^{\ddagger}$ = 5.9 kcal mol^{-1} via **TS D–E** (–8.4 kcal mol^{-1}) having a similar anionic allenic structure stabilized by the conjugation with the benzene ring ($\Delta G^{\ddagger}$ = 16.5 kcal mol^{-1} from **B**; Figure 1).[18] The strong *trans* influence of the silyl ligand on copper in **B** would facilitate the carbon–copper bond cleavage at its *trans*-position.[19] In the actual experimental system, the dissociated alkenyl anion equivalent should be stabilized by a nearby sodium cation (in the solvation form), but the calculations were performed without explicitly locating the sodium cation to simplify various possible local minima in ion-paired structures. A representative calculated pathway with the incorporation of a

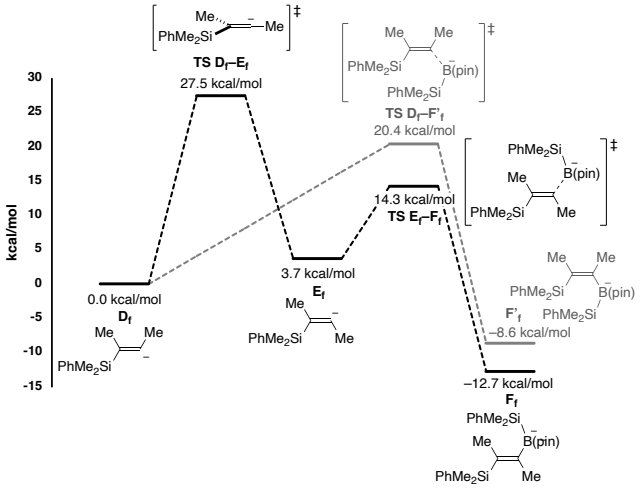

Scheme 5. Calculated reaction isomerization and borylation pathways for the reaction of **1f** with **2**.

sodium cation is shown in Scheme S2 in the Supporting Information. This isomerization mechanism is also consistent with the stereoselectivity switch for the reaction of dialkylacetylenes [Eq. (2)] because they cannot undergo such *syn*-to-*anti* isomerization via the allenic transition state due to the lack of an aromatic substituent for stabilization. In fact, we calculated the *syn*-to-*anti* isomerization pathway for the reaction of 2-butyne (**1f**) as a model dialkylacetylene (Scheme 5). As a result, the isomerization was found to go through a linear alkenyl anion transition state **TS D_f–E_f** with the energy barrier of $\Delta G^{\ddagger}$ = 27.5 kcal mol^{-1}, which is significantly higher than that for the direct borylation of *syn*-alkenyl anion **D_f** via **TS D_f–F'_f** ($\Delta G^{\ddagger}$ = 20.4 kcal mol^{-1}).[20]

The isomerized intermediate **E** in Scheme 3 reacts with silylboronate **2a** to form a carbon–boron bond via **TS E–F** (4.8 kcal mol^{-1}, $\Delta G^{\ddagger}$ = 17.4 kcal mol^{-1}), giving alkenyl(silyl)borate **F** (–15.1 kcal mol^{-1}). Subsequent transfer of the dimethylphenylsilyl group from boron to copper gives product *anti*-**3a** with regeneration of disilylcuprate **A** (–32.7 kcal mol^{-1}). In comparison, the reaction of **D** with **2a** toward the formation of *syn*-**3a** via intermediate **F'** (–9.9 kcal mol^{-1}) required the energy barrier of $\Delta G^{\ddagger}$ = 26.1 kcal mol^{-1} at the carbon–boron bond-forming **TS D–F'** (11.8 kcal mol^{-1}), which is significantly higher in energy than **TS E–F**. The overall energy profile matches well with the experimental results of selective formation of *anti*-**3a**, and the stereoselectivity of the product is determined at the borylation step with reversible *syn*/*anti* isomerization of the alkenyl nucleophile.

The origin of *anti*-selectivity for the reaction of **1a** with **2** is caused by the steric repulsion between the dimethylphenylsilyl group on the alkene and the incoming boryl group. Indeed, the bond angle of the alkene and the boron (∠C2–C1–B) of **TS E–F** is 121.2°, whereas that of **TS D–F'** is 135.9° and the silylboronate unit is distorted outside (Figure 2).[20] These computational results indicate that *anti*-borylation **TS E–F** is sterically more favored than *syn*-borylation **TS D–F'**, leading to the selective formation of *anti*-**3a**.

In this silylboration reaction, alkynes having a bulky alkyl substituent such as 3,3-dimethyl-1-phenyl-1-butyne (*tert*-

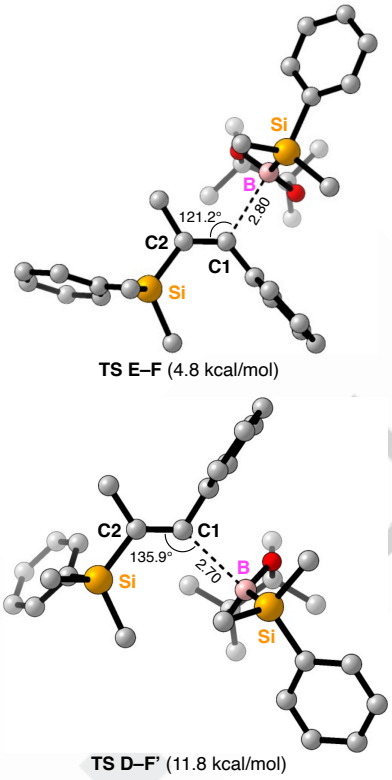

Figure 2. Structures of **TS E–F** and **TS D–F'**. Bond lengths are in Å.

butyl(phenyl)acetylene; **1c**) also gave *anti*-addition product *anti*-**3c** selectively as shown in Eq. (1). Even for this bulky substrate, the steric control toward *anti*-selective addition was found to be operative. Thus, the same structural analysis of the borylation transition states was performed and it was suggested that the formation of *anti*-**3c** is more favorable than *syn*-**3c** and each bond angle around the alkene is closer to 120° for the transition state toward *anti*-**3c** than that toward *syn*-**3c** (see Scheme S3 and Table S1 in the Supporting Information for details).

Conclusion

In summary, we theoretically examined the mechanism of a copper-catalyzed regio- and *anti*-selective 1,2-silylboration of alkyl(aryl)acetylenes to understand the reaction pathway and the origin of selectivity. As a result, we could elucidate the overall profile of this catalysis for the reaction of 1-phenyl-1-propyne (**1a**) with silylboronate **2**, and found that the regioselectivity is determined by both electronic and steric effects at the alkyne insertion step, and that the *syn*-to-*anti* isomerization takes place reversibly through an anionic allenic transition state stabilized by the existence of the benzene ring rather than a typical η^2-vinylmetal (metalacyclopropene) species. The *anti*-selectivity was found to be determined at the borylation step with the control by the steric effect of the silyl group introduced on the alkyne carbon. The importance of the aryl group on the alkyne to electronically induce *syn*-to-*anti* isomerization was further confirmed by conducting the reactions with dialkylacetylenes for comparison. The results obtained in this study would be highly informative for

the development of new catalytic transformations involving *syn*/*anti*-isomerization processes, which are currently under investigation in our laboratory.

Supporting Information

The authors have cited additional references within the Supporting Information.[21–23]

Acknowledgements

Support has been provided in part by JSPS KAKENHI Grant Numbers JP20H02741 (Grant-in-Aid for Scientific Research (B); R.S.) and JP22K05101 (Grant-in-Aid for Scientific Research (C); M.Y.), Toray Science Foundation (R.S.), and JST, the establishment of university fellowships towards the creation of science technology innovation, Grant Number JPMJFS2125 (H.M.).

Keywords: alkyne • copper • DFT calculation • mechanism • silylboronate

[1] For reviews: a) Y. K. Mirza, P. S. Bera, S. B. Mohite, A. K. Pandey, M. Bera, *Org. Chem. Front.* **2024**, *11*, 4290–4317; b) Y.-Y. Zhao, Y.-J. Jia, Y.-C. Hu, *Org. Chem. Front.* **2024**, *11*, 2351–2374; c) A. Torres-Calis, J. J. García, *ACS Omega* **2022**, *7*, 37008–37038; d) Y. Zheng, W. Zi, *Tetrahedron Lett.* **2018**, *59*, 2205–2213; e) A. M. Suess, G. Lalic, *Synlett* **2016**, *27*, 1165–1174.

[2] For reviews: a) Z. Yin, W. Shi, X.-F. Wu, *J. Org. Chem.* **2023**, *88*, 4975–4994; b) P. P. Pal, S. Ghosh, A. Hajra, *Org. Biomol. Chem.* **2023**, *21*, 2272–2294; c) J. Corpas, P. Mauleón, R. G. Arrayás, J. C. Carretero, *ACS Catal.* **2021**, *11*, 7513–7551; d) A. Whyte, A. Torelli, B. Mirabi, A. Zhang, M. Lautens, *ACS Catal.* **2020**, *10*, 11578–11622; e) W. Liu, W. Kong, *Org. Chem. Front.* **2020**, *7*, 3941–3955; f) A. Düfert, D. B. Werz, *Chem. Eur. J.* **2016**, *22*, 16718–16732; f) Y. Shimizu, M. Kanai, *Tetrahedron Lett.* **2014**, *14*, 3727–3737.

[3] a) V. W. Bhoyare, A. G. Tathe, A. Das, C. C. Chintawar, N. T. Patil, *Chem. Soc. Rev.* **2021**, *50*, 10422–10450; b) G. Fang, X. Bi, *Chem. Soc. Rev.* **2015**, *44*, 8124–8173; c) T. Besset, T. Poisson, X. Pannecoucke, *Eur. J. Org. Chem.* **2015**, 2765–2789.

[4] a) K. A. Brady, T. A. Nile, *J. Organomet. Chem.* **1981**, *206*, 299–304; b) I. Ojima, N. Clos, R. J. Donovan, P. Ingallina, *Organometallics* **1990**, *9*, 3127–3133; See also: c) D. W. Hart, J. Schwartz, *J. Organomet. Chem.* **1975**, *87*, C11–C14.

[5] a) R. S. Tanke, R. H. Crabtree, *J. Am. Chem. Soc.* **1990**, *112*, 7984–7989; b) Y. Miyake, E. Isomura, M. Iyoda, *Chem. Lett.* **2006**, *35*, 836–837; For a recent review: c) W. Gao, S. Ding, *Synthesis* **2020**, *52*, 3549–3563.

[6] a) D. Zell, C. Kingston, J. Jermaks, S. R. Smith, N. Seeger, J. Wassmer, L. E. Sirois, C. Han, H. Zhang, M. S. Sigman, F. Gosselin, *J. Am. Chem. Soc.* **2021**, *143*, 19078–19090; b) C. Shan, M. He, X. Luo, R. Li, T. Zhang, *Org. Chem. Front.* **2023**, *10*, 4243–4249; c) R. Chandrasekaran, K. Selvam, T. Rajeshkumar, T. Chinnusamy, L. Maron, R. Rasappan, *Angew. Chem. Int. Ed.* **2024**, *63*, e202318689.

[7] a) W. Lv, S. Liu, Y. Chen, S. Wen, Y. Lan, G. Cheng, *ACS Catal.* **2020**, *10*, 10516–10522; b) F. Zhou, W. Shi, X. Liao, Y. Yang, Z.-X. Yu, J. You, *ACS Catal.* **2022**, *12*, 676–686; c) X. Yan, M. Yang, Y.-B. She, Y.-F. Yang, *Dalton Trans.* **2023**, *52*, 737–746.

[8] B. Sánchez-Page, J. Munarriz, M. V. Jiménez, J. J. Pérez-Torrente, J. Blasco, G. Subias, V. Passarelli, P. Álvarez, *ACS Catal.* **2020**, *10*, 13334–13351.

[9] J. J. Pérez-Torrente, D. H. Nguyen, M. V. Jiménez, F. J. Modrego, R. Puerta-Oteo, D. Gómez-Bautista, M. Iglesias, L. A. Oro. *Organometallics* **2016**, *35*, 2410–2422.

[10] a) L. W. Chung, Y.-D. Wu, B. M. Trost, Z. T. Ball, *J. Am. Chem. Soc.* **2003**, *125*, 11579–11582; b) S. Ding, L.-J. Song, L. W. Chung, X. Zhang, J. Sun, Y.-D. Wu, *J. Am. Chem. Soc.* **2013**, *135*, 13835–13842.

[11] a) A. Kondoh, H. Yorimitsu, K. Oshima, *J. Am. Chem. Soc.* **2007**, *129*, 4099–4104; b) C. Che, H. Zheng, G. Zhu, *Org. Lett.* **2015**, *17*, 1617–1620; c) W. J. Jang, W. L. Lee, J. H. Moon, J. Y. Lee, J. Yun, *Org. Lett.* **2016**, *18*, 1390–1393; d) G. He, S. Qiu, H. Huang, G. Zhu, D. Zhang, R. Zhang, H. Zhu, *Org. Lett.* **2016**, *18*, 1856–1859; e) K. Nakamura, T. Nishikata, *ACS Catal.* **2017**, *7*, 1049–1052; f) J.-B. Tang, J.-Q. Bian, Y.-S. Zhang, Y.-F. Cheng, H.-T. Wen, Z.-L. Yu, Z.-L. Li, Q.-S. Gu, G.-Q. Chen, X.-Y. Liu, *Org. Lett.* **2022**, *24*, 2536–2540; g) X. Wang, H. Zeng, W. Zhang, H. Guo, T. Jin, S. Shi, X. Jin, N. Qu, L. Liu, L. Zhang, *Org. Biomol. Chem.* **2022**, *20*, 7949–7955; h) F. Tang, Y.-S. Feng, Z.-F. Cheng, Q. Zhang, H.-J. Xu, *Org. Lett.* **2023**, *25*, 3916–3921; i) A. Maity, A. K. Sahoo, *J. Org. Chem.* **2024**, *89*, 852–863.

[12] a) H. Moniwa, R. Shintani, *Chem. Eur. J.* **2021**, *27*, 7512–7515; See also: b) T. Ohmura, Y. Takaoka, M. Suginome, *Chem. Commun.* **2021**, *57*, 4670–4673; c) R. Kondo, H. Moniwa, R. Shintani, *Org. Lett.* **2023**, *25*, 4193–4197.

[13] For reviews on silylboronates: a) J.-J. Feng, W. Mao, L. Zhang, M. Oestreich, *Chem. Soc. Rev.* **2021**, *50*, 2010–2073; b) J. R. Wilkinson, C. E. Nuyen, T. S. Carpenter, S. R. Harruff, R. Van Hoveln, *ACS Catal.* **2019**, *9*, 8961–8979; c) M. Oestreich, E. Hartmann, M. Mewald, *Chem. Rev.* **2013**, *113*, 402–411; d) T. Ohmura, M. Suginome, *Bull. Chem. Soc. Jpn.* **2009**, *82*, 29–49.

[14] Gaussian 16, Revision C.01, M. J. Frisch, G. W. Trucks, H. B. Schlegel, G. E. Scuseria, M. A. Robb, J. R. Cheeseman, G. Scalmani, V. Barone, G. A. Petersson, H. Nakatsuji, X. Li, M. Caricato, A. V. Marenich, J. Bloino, B. G. Janesko, R. Gomperts, B. Mennucci, H. P. Hratchian, J. V. Ortiz, A. F. Izmaylov, J. L. Sonnenberg, D. Williams-Young, F. Ding, F. Lipparini, F. Egidi, J. Goings, B. Peng, A. Petrone, T. Henderson, D. Ranasinghe, V. G. Zakrzewski, J. Gao, N. Rega, G. Zheng, W. Liang, M. Hada, M. Ehara, K. Toyota, R. Fukuda, J. Hasegawa, M. Ishida, T. Nakajima, Y. Honda, O. Kitao, H. Nakai, T. Vreven, K. Throssell, J. A. Montgomery, Jr., J. E. Peralta, F. Ogliaro, M. J. Bearpark, J. J. Heyd, E. N. Brothers, K. N. Kudin, V. N. Staroverov, T. A. Keith, R. Kobayashi, J. Normand, K. Raghavachari, A. P. Rendell, J. C. Burant, S. S. Iyengar, J. Tomasi, M. Cossi, J. M. Millam, M. Klene, C. Adamo, R. Cammi, J. W. Ochterski, R. L. Martin, K. Morokuma, O. Farkas, J. B. Foresman, D. J. Fox, Gaussian, Inc., Wallingford CT, 2019.

[15] a) A. D. Becke, *J. Chem. Phys.* **1993**, *98*, 5648–5652; b) C. Lee, W. Yang, R. G. Parr, *Phys. Rev. B* **1998**, *37*, 785–789; c) P. J. Stephens, F. J. Devlin, C. F. Chabalowski, M. J. Frisch, *J. Phys. Chem.* **1994**, *98*, 11623–11627.

[16] A. V. Marenich, C. J. Cramer, D. G. Truhlar, *J. Phys. Chem. B* **2009**, *113*, 6378–6396.

[17] H. Moniwa, M. Yamanaka, R. Shintani, *J. Am. Chem. Soc.* **2023**, *145*, 23470–23477.

[18] a) D. Y. Curtin, J. W. Crump, *J. Am. Chem. Soc.* **1958**, *80*, 1922–1926; b) R. Knorr, T. Menke, C. Behringer, K. Ferchland, J. Mehlstäubl, E. Lattke, *Organometallics* **2013**, *32*, 4070–4081; c) H. Yamaguchi, F. Takahashi, T. Kurogi, H. Yorimitsu, *Synthesis* **2024**, *56*, DOI: 10.1055/a-2326-6416.

[19] a) R. N. Haszeldine, R. V. Parish, J. H. Setchfield, *J. Organomet. Chem.* **1973**, *57*, 279–285; b) P. N. Kapoor, R. Kakkar, *J. Mol. Struct. (Theochem)* **2004**, *679*, 149–156; See also: c) J. Gao, Y. Ge, C. He, *Chem. Soc. Rev.* **2024**, *53*, 4648–4673.

[20] See the Supporting Information for more details.

[21] M. Suginome, T. Matsuda, H. Nakamura, Y. Ito, *Tetrahedron* **1999**, *55*, 8787–8800.

[22] a) S. R. Allen, R. G. Beevor, M. Green, N. C. Norman, A. G. Orpen, I. D. Williams, *J. Chem. Soc., Dalton Trans*. **1985**, 435–450; b) D. S. Frohnapfel, J. L. Templeton, *Coord. Chem. Rev.* **2000**, *206–207*, 199–235; c) D. C. Brower, K. R. Birdwhistell, J. L. Templeton, J. L. *Organometallics* **1986**, *5*, 94–98.

[23] a) F. M. Bickelhaupt, *J. Comput. Chem.* **1999**, *20*, 114–128; b) F. M. Bickelhaupt, K. N. Houk, *Angew. Chem. Int. Ed*. **2017**, *56*, 10070–10086; c) B. J. Levandowski, K. N. Houk, *J. Org. Chem.* **2015**, *80*, 3530–3537.

Entry for the Table of Contents

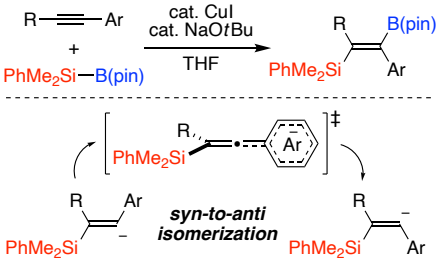

The mechanism of a copper-catalyzed regio- and *anti*-selective 1,2-silylboration of internal alkynes was theoretically examined. The overall reaction profile was proposed, and the *syn*-to-*anti* isomerization was found to take place through an anionic allenic transition state stabilized by the benzene ring. The *anti*-selectivity was determined at the borylation step and controlled by the steric effect.